# Towards Robust High Speed Underwater Acoustic Communications Using Chirp Multiplexing

Jiacheng Shi, Emrecan Demirors, and Tommaso Melodia
Department of Electrical and Computer Engineering, Northeastern University, Boston, MA 02115
E-mail:{shijc, edemirors, melodia}@ece.neu.edu

***Abstract*—Wide band chirp spread spectrum (CSS) has been studied in underwater acoustic (UWA) communications to guarantee low bit error rates with low transmission rates. On the other hand, high speed transmission schemes for UWA, especially Orthogonal-Frequency-Division-Multiplexing (OFDM) technology, can reach Mbit/s data rates but at the expense of reliability. In this paper, we propose a new transmission scheme based on multiplexing information bits to (quasi-)orthogonal chirp signals, called Quasi-Orthogonal Chirp Multiplexing (QOCM). It can be easily implemented on reprogrammable hardware as an extension to OFDM architectures. We evaluated the performance of the proposed scheme with simulation and tank experiments. Results show that QOCM scheme is able to achieve one order of magnitude better performance than an OFDM scheme under severe Doppler effect posed by simulation in long distance water transmission. Moreover, we observe in water tank experiment that the QOCM scheme is resilient against to the Doppler effects induced by relative speeds up to $5\,\mathrm{knots}$, which corresponds to a Doppler shift of $214.16\,\mathrm{Hz}$ at a center frequency of $125\,\mathrm{kHz}$.**

***Index Terms*—Underwater acoustic communications, chirp multiplexing, robust.**

## I. Introduction

Underwater acoustic channel is temporally and spatially varying, which poses significant challenges on the underwater acoustic (UWA) communication systems, including limited bandwidth, multi-path, large attenuation, Doppler spread, and propagation delay [1] [2]. To address these challenges, researchers have been exploring different communication schemes to achieve reliable yet high rate communications. For example, chirp signals have been leveraged quite often to achieve high reliability in UWA communications [3]–[5]. A chirp is a signal of which the frequency varies in time. Wide band chirp signal with high processing gain (duration bandwidth product) has proven to overcome multipath and Doppler shifts even at low signal-to-noise ratio (SNR) conditions [6]. However, consequently, wide band chirp signals can usually achieve low data rates (up to few $\mathrm{kbit/s}$) [3]. Different schemes that use wide band chirps are also proposed. In [5], a chirp-based code-time-frequency spanning scheme is proposed and tested, where they present bit-error rate (BER) performances up to $10^{-6}$ with $0\,\mathrm{dB}$ SNR. An M-ary chirp spread signal (MCSS) schemes is presented in [4]. While these schemes offer promising results in terms of reliability, they can only support data rates of few $\mathrm{kbit/s}$.

**Acknowledgement:** This work was supported by the National Science Foundation under Grant CNS-1503609 and Grant CNS-1726512.

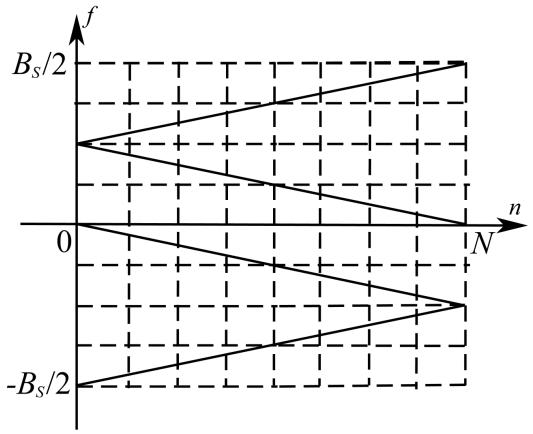


Fig. 1: An example of $M = 4$ chirp subcarriers with $N = 8$ samples per subcarrier and processing gain $K = 2$. The figure shows the frequency changes of each subcarrier over time index $n$. The information bits for this transmission are 0,1,1,0.

On the other hand, to increase data rate and bandwidth efficiency, Orthogonal-Frequency-Division-Multiplexing (OFDM) technology has been widely adopted in UWA communications [7]–[11]. In [8], an adaptive OFDM Modulation scheme is proposed to reduce the frequency offset by adaptively adjusting power allocation using the feedback from channel estimation. [12] presents a reconfigurable underwater networking platform that aims to support high data rate by leveraging OFDM based modulation schemes. The former works are proved to achieve data rates up to $1\mathrm{Mbit/s}$, while they can generally reach BER performances less than $10^{-5}$.

Consequently, chirp multiplexing is the answer to achieve both the goals. In radio frequency (RF) and optical domain, a few approaches to chirp multiplexing have been presented at much higher frequency bands. A multi-code ultra wide band chirp modulation scheme is proposed in [13]. The transmitted signal is designed as a summation of envelope shaped quasi-orthogonal chirp signals, and the receiver decodes with a series of match filters. In [14], Orthogonal Chirp Division

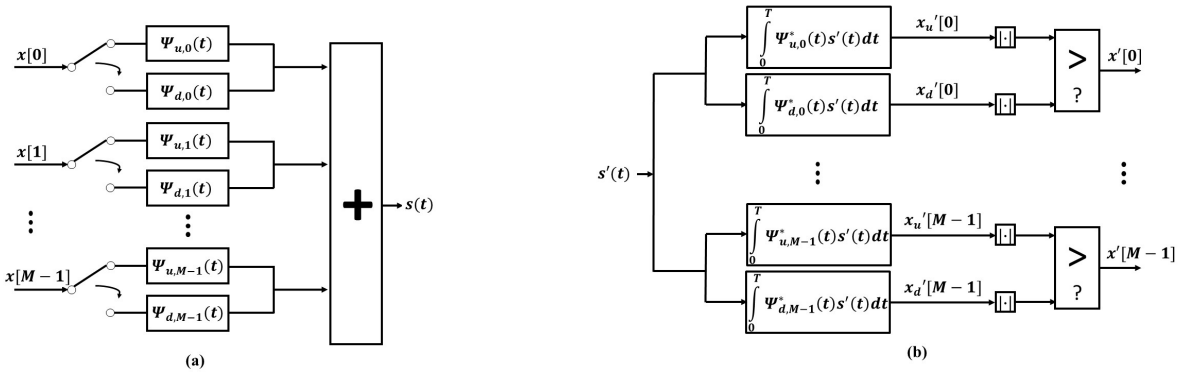


Fig. 2: Schematic diagrams of QOCM. (a) transmitter; (b) receiver.

Multiplexing (OCDM) is put forward by performing Discrete Fresnel Transform (DFnT) [15], which is equivalent to Discrete Fourier Transform (DFT) with additional phase shifts in both time and frequency domain. Both schemes apply (quasi-)orthogonal chirp signals as subcarriers to overcome multipath. However, match filters in [13] are hard to be implemented on hardware. Also, OCDM requires precise channel compensation.

In this paper, we propose a novel modulation scheme based on Quasi-Orthogonal Chirp Multiplexing (QOCM). We first introduce the basic complex chirp signal. Then we extend the basic chirp to two sets of mutually orthogonal chirp signals, which are used as subcarriers for the transmission. We provide the transmitter and receiver design and digital implementation of QOCM. Simulation and tank experiment results show that QOCM has high robustness and high data rate.

The rest of this paper is organized as follows. In Section 2, we present the architecture of the QCOM system. Then in Section 3, we provide the digital implementation of QOCM and compare it with OFDM systems. We present simulation and experimental results conducted in a water tank in Section 4. Finally, we draw the main conclusions in Section 5.

## II. System model

We propose a novel linear chirp based transmission scheme that uses a frequency hopping pattern. A chirp signal is defined as a frequency changing signal with a starting frequency $f_0$ and a final frequency $f_1$. The complex chirp waveform in each time period $T$ can be expresses as

$$c(t) = \exp(j2\pi f_0 t + j\pi\mu t^2) \tag{1}$$

where $j$ is the imaginary unit, and $\mu = \frac{f_1 - f_0}{T}$ is the frequency sweeping rate. When $\mu > 0$, we call $c(t)$ an up-chirp; when $\mu < 0$, we call $c(t)$ a down-chirp. The bandwidth of $c(t)$ can be expressed as $B_x = |f_1 - f_0|$.

The *processing gain* of a chirp signal is defined as its time-bandwidth product. In wide band chirp spread spectrum (CSS), chirp signals with higher processing gain are more resilient to frequency offset [6]. Furthermore, up and down chirps with the same duration and bandwidth, and higher processing gain have smaller inner product, which provides the property of quasi-orthogonality.

We first look into $M$ orthogonal up chirp codes $\{\psi_{u,m}(t)\}(m = 0, 1, \cdots, M-1)$ . For simplicity, we only discuss orthogonal chirps with uniformly increased stating frequencies and same sweeping rate $\mu_c = \Delta f/T$. Thus, the $m$-th chirp code is expressed as

$$\psi_{u,m}(t) = \exp(j2\pi m B_c t + j\pi\mu_c t^2) \tag{2}$$

where $B_c$ is the interval of the starting frequencies, $\mu_c$ is the sweeping rate. When $B_c T$ is an integer, the inner product of $\psi_{u,m}(t)$ and $\psi_{u,k}(t)$ can be found as $\delta(m-k)$, where $\delta(\cdot)$ is the Kronecker delta function. It indicates that the up chirp codes are mutually orthogonal. Correspondingly, We have $M$ orthogonal down chirps with the same absolute value of sweeping rate as up chirps but negative. The down chirps can be expressed as

$$\psi_{d,m}(t) = \exp(j2\pi(m+1) B_c t - j\pi\mu_c t^2) \tag{3}$$

The reason for choosing the starting frequency as $(m+1)B_c$ instead of $mB_c$ for the $m$-th down chirp is to avoid the frequency overlapping between the $(m-1)$-th up chirp and the $m$-th down chirp. As a result, the spectrum efficiency and the quasi-orthogonality of up and down chirps are improved.

All the up and down chirp signals form the subcarriers of Quasi-Orthogonal Chirp Multiplexing (QOCM). For the $M$ binary symbols $\{x[0], x[1], \ldots, x[M-1]\}, x[i] = 0$ or 1, we multiplex 1s to up chirps and 0 to down chirps. The 1s and 0s can be modulated as

$$s_u(t) = \frac{1}{M}\sum_{m=0}^{M-1} x_u[m]\exp(j2\pi m B_c t + j\pi\mu_c t^2) \tag{4}$$

$$s_d(t) = \frac{1}{M}\sum_{m=0}^{M-1} x_d[m]\exp(j2\pi(m+1) B_c t - j\pi\mu_c t^2) \tag{5}$$

where $x_u[m] = x[m]$, $x_d[m] = 1 - x[m]$, meaning that we send $\psi_{u,m}(t)$ when $x[m] = 1$; we send $\psi_{d,m}(t)$ when $x[m] = 0$. Then we have the signal for transmission $s(t) = s_u(t) + s_d(t)$.

At the receiver side, synchronization is necessary for precise

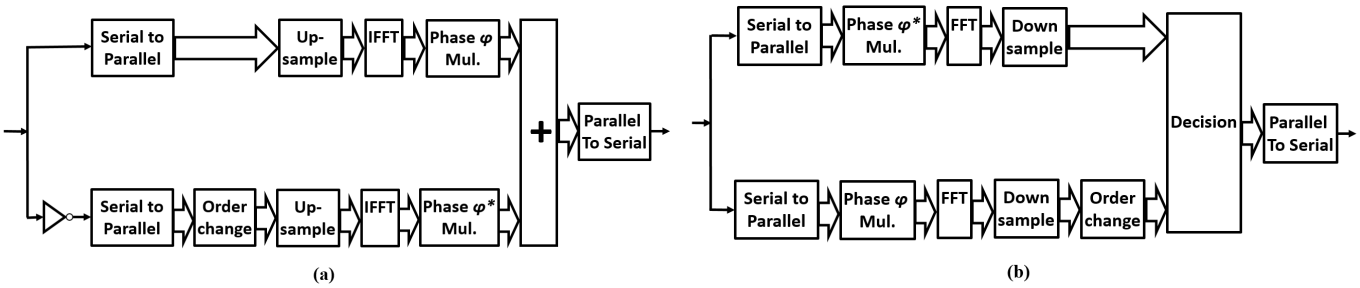


Fig. 3: Digital implementation of QOCM.(a) transmitter; (b) receiver.

decoding. We send a predefined $m$-sequence as a preamble. The receiver will correlate the preamble and the received signal. The position of the correlation peak indicates the start time of the code.

By applying the (quasi-)orthogonality, the receiver decodes the signal by correlating with each chirp code. To demodulate, we calculate the inner product with each up and down chirp code respectively.

$$x'_u[m] = \int_0^T s'(t)\text{exp}(-j2\pi m B_c t - j\pi\mu_c t^2)\text{d}t \quad (6)$$

$$x'_d[m] = \int_0^T s'(t)\text{exp}(-j2\pi (m+1) B_c t + j\pi\mu_c t^2)\text{d}t \quad (7)$$

where $s'(t)$ is the received signal. We make hard decision by comparing the amplitudes of $x'_u[m]$ and $x'_d[m]$. When $|x'_u[m]| \geq |x'_d[m]|$, we determine the $m$-th bit $x'[m] = 1$; otherwise, we determine $x'[m] = 0$.

The schematic diagrams of QOCM transmitter and receiver are shown in Figure 2.

## III. Digital Implementation

Here we propose an efficient and simple digital implementation of the transmitter and receiver of QOCM. Let $T_s$ be the sample time of the chirp signal. The signal occupies the bandwidth from $-B_s/2$ to $B_s/2$, where $B_s = 1/T_s$. The number of samples is $N = T/T_s$, and the continuous time variable becomes discrete variable $n = t/T_s, n = 0, 1, \cdots, N-1$. The resolution in the frequency domain is $B_s/N = 1/(NT_s)$. For simplicity, we assume that $B_c = L \cdot (B_s/N)$ ,where $L$ is an integer. For each chirp signal, the processing gain $K = \Delta f \cdot T$.

### A. Transmitter and Receiver Implementation

There is a difference between the continuous time signal and discrete time signal in the sense of frequency band. Under the same assumption that the bandwidth of the transmitted signal is $B_s$, the continuous signal occupies the band from 0 to $B_s$. The reason for the band shift is that the spectrum of discrete time signal is a periodic extension of the corresponding continuous time signal. When the frequency is over $B_s/2$, the spectra is shifted to the negative half. Fortunately, the total bandwidth $B_s$ and the orthogonality remain the same.

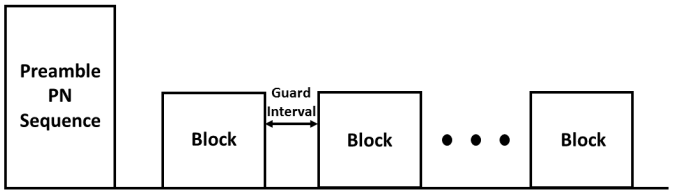


Fig. 4: Structure of the transmission data packet

An example of $N = 8$ samples per chirp with $L = 2$ and $K = 2$ is shown in Figure 1.

We first introduce up-sampled $x_u[m]$ and $x_d[m]$ as

$$\hat{x}_u[l] = \begin{cases} x_u[m] & l = Lm \\ 0 & \text{otherwise} \end{cases} \quad (8)$$

$$\hat{x}_d[l] = \begin{cases} x_d[M-1] & l = 0 \\ x_d[m] & l = L(m+1), m \neq M-1 \\ 0 & \text{otherwise} \end{cases} \quad (9)$$

Due to the limit of bandwidth, the number of codes $M$ is restricted to $M \leq N/L$. Thus (4) and (5) can be written as

$$s_u[n] = \frac{N}{M}\left(\frac{1}{N}\sum_{l=0}^{N-1}\hat{x}_u[l]\text{exp}(j2\pi\frac{ln}{N})\right)\cdot\text{exp}(j\pi\frac{Kn^2}{N^2}) \quad (10)$$

$$s_d[n] = \frac{N}{M}\left(\frac{1}{N}\sum_{l=0}^{N-1}\hat{x}_d[l]\text{exp}(j2\pi\frac{ln}{N})\right)\cdot\text{exp}(-j\pi\frac{Kn^2}{N^2}) \quad (11)$$

Noticing that the first parts of (10) and (11) is the inverse Discrete Fourier Transform (IDFT) of $\hat{x}_u[l]$ and $\hat{x}_d[l]$, the transmitter can be implemented by taking IFFT if of $\hat{x}_u[l]$ and $\hat{x}_d[l]$ and multiplication with different phase shift respectively. The phase shift for up chirp modulation is defined as

$$\phi[n] = \text{exp}(j\pi\frac{Kn^2}{N^2}) \quad (12)$$

For down chirp modulation, the phase shift becomes $\phi^*[n]$. We know that IDFT maps the data to a bunch of monotone complex sinusoidal waves. The physical meaning of the phase shift $\phi[n]$ is to shape the sinusoidal signals to chirp signals with the same bandwidth.

Similarly, at the receiver side, (6) and (7) in discrete time

can be derived as

$$\hat{x}'_u[l] = \sum_{n=0}^{N-1} \left( s'[n] \text{exp}(-j\pi \frac{Kn^2}{N^2}) \text{exp}(j2\pi \frac{ln}{N}) \right) \quad (13)$$

$$\hat{x}'_d[l] = \sum_{n=0}^{N-1} \left( s'[n] \text{exp}(j\pi \frac{Kn^2}{N^2}) \text{exp}(j2\pi \frac{ln}{N}) \right) \quad (14)$$

That is, the received signal first multiplies with $\phi^*[n]$ or $\phi[n]$ in time domain. The chirp signals will be shifted "back" to sinusoidal signals. After performing DFT, pulses will appear at the starting frequencies of chirp. Finally, we need to downsample the result by $L$ respectively.

$$x'_u[m] = \hat{x}'_u[l], l = Lm \quad (15)$$

$$x'_d[m] = \begin{cases} \hat{x}'_d[l] & l = L(m+1), m \neq M-1 \\ \hat{x}'_d[0] & m = M-1 \end{cases} \quad (16)$$

The decision $x'[m]$ is made by comparing the $|x'_u[m]|$ and $|x'_d[m]|$. Figure 3 presents the flow chart of QOCM digital implementation.

### B. Packetization

We setup the transmission data packet in a zero padding (ZP)-OFDM style. To encode the information bits, we employ IFFT and phase shift to map the bits to up or down chirps. This forms a transmission block. Afterwards, guard intervals are inserted between the blocks. Finally, a PN sequence is added to the beginning of the signal as a preamble for the receiver to perform the synchronization. The structure of the packet is shown in Figure 4.

At the receiver side, we first correlate the received signal with the predefined PN sequence for synchronization. This is to determine the position of the blocks. Then we take the inverse operation of multiplexing for each block, that is to employ the phase shift and FFT for both up and down chirps. Finally, we downsample the data and make the decision by comparing the amplitude of the decoded signal.

### C. Comparison with OFDM

We compare QOCM system with OFDM system. QCDM system generates a set of (quasi-)orthogonal chirp signals, like IFFT in OFDM generates a set of orthogonal sinusoidal signals. QOCM can be regarded as a two-step process including IFFT/FFT. It can be easily implemented on hardware with OFDM system without significantly changing the design. In fact, OFDM is a special case of the chirp that the processing gain of each "chirp" is 0.

In QOCM, each information bit is mapped to either an up chirp or a down chirp signal. In other words, one 'symbol' (up or down chirp) represents one information bit. This is similar to the BPSK modulation in OFDM. BPSK symbols contain amplitude and phase information. We need to consider the influence of the channel and perform the equalization based on channel estimation [7] to precisely decode BPSK symbols. However, for up and down chirp mapping, we make the decision based on the relative amplitude only. No channel estimation is required.

In fact, we can add amplitude and phase information to the up and down chirp signals, like PSK or QAM, to further increase the data rate. However, in this case, channel estimation and compensation will be necessary to find the absolute values of amplitude and phase rather than the relativity. This is left for future work.

## IV. Performance Evaluation

We present the performance evaluation of the proposed QOCM scheme. To that end, first we compare the performance of QOCM with different parameters against OFDM in terms of bit-error rate (BER) performance in simulation and then we provide quantitative proof for Doppler resilience of the QOCM through tank test experiments.

### A. BER vs SNR simulation

In the simulation, we used a bandwidth of $B = 7.81\,\text{kHz}$ with a carrier frequency of $fc = 50\,\text{kHz}$. For the channel, we use the statistical channel model in [16] with acoustic noise

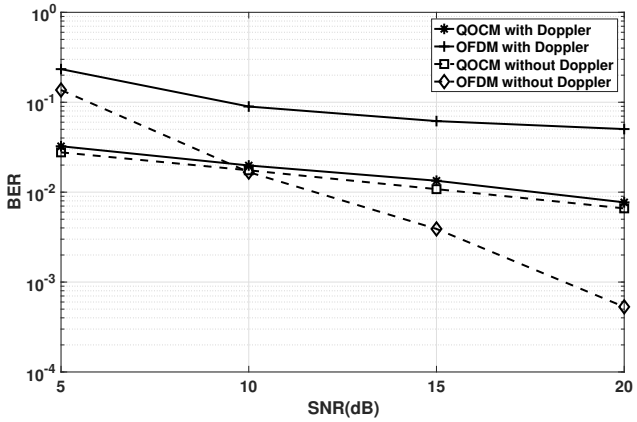


Fig. 5: BER performance versus SNR.

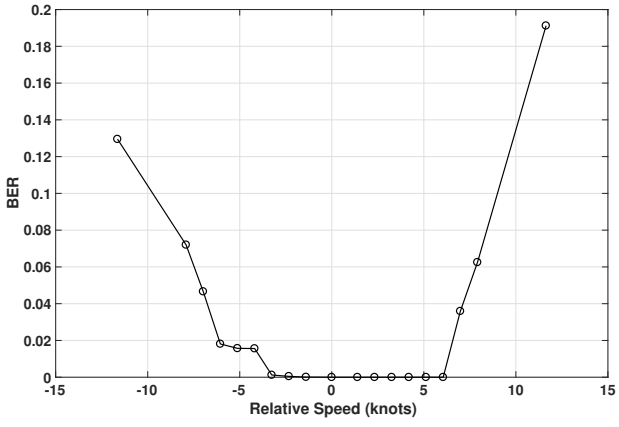


Fig. 6: BER performance versus relative speed.

calculations [1]. In simulations, we considered one transmitter and one receiver node that are $1\,\mathrm{km}$ apart from each other at a depth of $20\,\mathrm{m}$, with total depth of $100\,\mathrm{m}$. We also generated Doppler effect by applying frequency drift on transmitter and receiver at 200Hz and 50Hz respectively. We compare the performance of the QOCM with 128 subcarriers and OFDM with 256 subcarriers (half of them are used as pilots) using BPSK scheme over the same bandwidth $B$. As a result, the data rate of the two transmissions are $39.1\,\mathrm{kbit/s}$ with a symbol duration of $3.28\,\mathrm{ms}$. Figure 5 shows the BER as a function of the received SNR. We observe that, in the presence of a Doppler effect, the proposed QOCM offers better BER performance compared to the OFDM. In the case where there is no Doppler effect, the proposed QOCM performs better than OFDM in lower SNRs (lower than $10\,\mathrm{dB}$).

### *B. Doppler Effect.*

We conducted a series of experiments in a water test tank of dimensions $2.5\,\mathrm{m} \times\ 2\,\mathrm{m} \times\ 1\,\mathrm{m}$, where we deployed two software-defined underwater acoustic modems [9], [11]. We evaluate the performance of QOCM with 64 subcarriers over a bandwidth of $B = 97.656\,\mathrm{kHz}$ and at a carrier frequency of $fc = 125\,\mathrm{kHz}$ in terms of BER under different Doppler conditions. To realize that, we synthetically introduced Doppler effect to the received signals, which corresponds to different relative speeds. Figure 6 shows the BER as a function of the relative speed. We observe that performance degradation is limited for relative speeds up to $5\,\mathrm{knots}$, which corresponds to a Doppler shift of $214.16\,\mathrm{Hz}$ at a center frequency of $125\mathrm{kHz}$. This proves that the proposed communication scheme is resilient against relatively severe Doppler effects.

## V. Conclusion

In this paper, we proposed a novel transmission scheme based on orthogonal chirp signals aiming at higher data rate and lower error rate. First, we introduced two sets of (quasi-)orthogonal chirp signals. Then we designed the QOCM transmitter and receiver in continuous time, which takes advantage of the (quasi-)orthogonality of up and down chirp signals. Moreover, we provided the digital implementation of QOCM. It can be easily extended from existing OFDM implementation. Finally, we presented a set of simulation and experimental results showing QOCM is more resilient against Doppler effect compared to OFDM.

## References


[1] T. Melodia, H. Kulhandjian, L. Kuo, and E. Demirors, "Advances in Underwater Acoustic Networking," in *Mobile Ad Hoc Networking: Cutting Edge Directions*, 2nd ed., S. Basagni, M. Conti, S. Giordano, and I. Stojmenovic, Eds. Inc., Hoboken, NJ: John Wiley and Sons, 2013, pp. 804–852.

[2] M. Stojanovic, *Acoustic (underwater) Communications*, J. G. Proakis, Ed. Hoboken, NJ: John Wiley and Sons, Inc., 2003.

[3] L. LeBlanc, M. Singer, P.-P. Beaujean, C. Boubli, and J. Alleyne, "Improved chirp FSK modem for high reliability communications in shallow water," in *OCEANS 2000 MTS/IEEE Conference and Exhibition*, vol. 1, 2000, pp. 601–603.

[4] W. Lei, D. Wang, Y. Xie, B. Chen, X. Hu, and H. Chen, "Implementation of a high reliable chirp underwater acoustic modem," in *Oceans, 2012-Yeosu*, Yeosu, South Korea, 2012, pp. 1–5.

[5] E. Demirors and T. Melodia, "Chirp-Based LPD/LPI Underwater Acoustic Communications with Code-Time-Frequency Multidimensional Spreading," in *Proc. of ACM Intl. Conf. on Underwater Networks & Systems (WUWNet)*, Shanghai, China, October 2016.

[6] X. Lurton, *An Introduction to Underwater Acoustics: Principles and Applications*, ser. Springer Praxis Books. Springer.

[7] S. Zhou and Z. Wang, *OFDM for underwater acoustic communications*. John Wiley & Sons, 2014.

[8] A. Radosevic, R. Ahmed, T. Duman, J. Proakis, and M. Stojanovic, "Adaptive OFDM modulation for underwater acoustic communications: Design considerations and experimental results," *IEEE Journal of Oceanic Engineering*, vol. 39, no. 2, pp. 357–370, 2014.

[9] E. Demirors, G. Sklivanitis, T. Melodia, S. N. Batalama, and D. A. Pados, "Software-defined underwater acoustic networks: toward a high-rate real-time reconfigurable modem," *IEEE Communications Magazine*, vol. 53, no. 11, pp. 64–71, November 2015.

[10] E. Demirors, B. G. Shankar, G.E. Santagati and T. Melodia, "SEANet: A Software-Defined Acoustic Networking Framework for Reconfigurable Underwater Networking," in *Proc. of ACM Intl. Conf. on Underwater Networks & Systems (WUWNet)*, Washington, DC, November 2015.

[11] E. Demirors, G. Sklivanitis, G. E. Santagati, T. Melodia, and S. N. Batalama, "A high-rate software-defined underwater acoustic modem with real-time adaptation capabilities," *IEEE Access*, vol. PP, no. 99, pp. 1–1, 2018.

[12] E. Demirors, J. Shi, R. Guida and T. Melodia, "SEANet G2: A Toward a High-Data-Rate Software-Defined Underwater Acoustic Networking Platform," in *Proc. of ACM Intl. Conf. on Underwater Networks & Systems (WUWNet)*, Shanghai, China, October 2016.

[13] H. Liu, "Multicode ultra-wideband scheme using chirp waveforms," *IEEE Journal on selected areas in communications*, vol. 24, no. 4, pp. 885–891, 2006.

[14] X. Ouyang and J. Zhao, "Orthogonal chirp division multiplexing," *IEEE Transactions on Communications*, vol. 64, no. 9, pp. 3946–3957, 2016.

[15] I. Aizenberg and J. T. Astola, "Discrete generalized fresnel functions and transforms in an arbitrary discrete basis," *IEEE transactions on signal processing*, vol. 54, no. 11, pp. 4261–4270, 2006.

[16] P. Qarabaqi and M. Stojanovic, "Statistical characterization and computationally efficient modeling of a class of underwater acoustic communication channels," *IEEE Journal of Oceanic Engineering*, vol. 38, no. 4, pp. 701–717, 2013.